



# Optimization of fermentation conditions using response surface methodology (RSM) with kinetic studies for the production of bioethanol from rejects of *Kappaphycus alvarezii* and solid food waste

P. Priyadharsini<sup>1,2</sup> · S. S. Dawn<sup>1,3</sup>

Received: 26 May 2021 / Revised: 22 July 2021 / Accepted: 26 July 2021 / Published online: 24 August 2021  
© The Author(s), under exclusive licence to Springer-Verlag GmbH Germany, part of Springer Nature 2021

## Abstract

*Kappaphycus alvarezii* reject (KR) and solid food waste (SFW) are unused sources of carbohydrates; the production of bioethanol from these raw materials has not yet been reported by any researchers so far. The present study was conducted to optimize the fermentation parameters using RSM (Design-Expert version 7.0 software). KR and SFW were fermented by using *Saccharomyces cerevisiae* for bioethanol production. Logistic and modified Gompertz kinetic models were fitted fermentation time against bioethanol yield data. The gas chromatography flame ionization detector (GC–FID) was used for bioethanol confirmation. The optimum conditions for an incubation time of 24 h, inoculum size of 15 vol%, and agitation speed of 90 rpm at pH 5 were predicted by RSM. Under these experimental conditions, the best yield of bioethanol was 68% (w/w), which is in good agreement with the predicted value from RSM of 70% (w/w) with an  $R^2$  of 0.97. Under the optimized conditions, the reducing sugar reduced from 30.83 to 8.55 g/L with a conversion efficiency of 70%. Overall, KR and SFW were effective resources for the production of bioethanol to meet the future energy demand. The diversion of SFW through their study will provide a breakthrough for the reduction of energy potential SFW to landfills, contributing to the climate change initiative.

**Keywords** *Kappaphycus alvarezii* reject · Solid food waste · Fermentation · Response surface methodology · Bioethanol

## 1 Introduction

Seaweeds are macroalgae; based on the color and biochemical composition, they are broadly classified into red, brown, and green algae. Almost 7.5–8 million tonnes of seaweed are harvested worldwide per annum. These macroalgae are enormously found on the east and west coastline of India [1]. In 2016, nearly 22,000 tonnes of seaweed were harvested from Indian coastal lines. This was only 2.5% of 870,000

tonnes of seaweed available on the Indian coastal line. Seaweeds serve as resource for variety of industrially valuable products such as Carrageenan, alginates, agar, and biofuels [2]. In industries, during recovery of valuable products, a tremendous quantity of algal rejects is produced worldwide. Disposal of these algal rejects are challenging and highly demandable. Many of the marine algae processing industries primarily convert the algae rejects into fertilizer via bio-processing techniques [3]. Khamathy et al. proved KR to be an eligible source for bioethanol production [4]. In the current scenario, globally many research groups are engaged in converting waste to bioenergy products. Owing to renewable and sustainable energy usage, waste diversion to biofuels is more recommended than other conversion processes [2, 3].

Food waste is an organic waste that is produced from sources such as households, cafes, and restaurants on a day to day basis. About 1.3 billion tonnes of food gets wasted in the food supply chain [5]. Food waste disposal current techniques raise concern for environmental safety as well

✉ S. S. Dawn  
dawnsudha@yahoo.com

<sup>1</sup> Centre of Excellence for Energy Research, Sathyabama Institute of Science and Technology, Chennai 600 119, India

<sup>2</sup> Department of Chemistry, Sathyabama Institute of Science and Technology, Chennai 600 119, India

<sup>3</sup> Centre for Waste Management, Sathyabama Institute of Science and Technology, Tamil Nadu, Chennai 600 119, India

as protection of natural wealth. Presently, such food wastes are disposed through a number of processes, namely dumping on landfills, incineration, and burial etc. These methods are less recommended, as they release hazardous gases into the atmosphere and contaminate the ground water [6, 7]. These drawbacks necessitate safer disposal of food waste. Also, the food waste composition (starch and cellulose) favors recovery of valuable products [8]. The carbohydrate content present in the food waste can be used for production of bioethanol through fermentation process. [9]. Also several studies have been reported on the conversion of food waste into biogas and methane [10–12]. Anaerobic digestion of rice straw, rice bran, and food waste resulted in a methane yield of 235.4 mL/g-VS at the fifth day of incubation time [13], while a few others have reported food waste as a source for the synthesis of economically viable adsorbent, i.e., activated carbon [14].

Fossil fuel usage in the last decades resulted in global climatic change, CO<sub>2</sub> emissions, fuel insecurity, and higher fuel cost [15]. Plants, algal reject waste, food waste, and agricultural or forestry residues are the main sources for bio-fuel production [16, 17]. Among the biofuels, bioethanol is one of the green energy sources and has become more generally embraced as an alternative to fossil fuel [2]. Sudhakar et al. reported seaweed reject (*Gracilaria corticata*) provides 3.75% w/w ethanol (72 h, pH 5.5) using *Saccharomyces cerevisiae* [18]. From food waste (hamburger), 0.271 g/L of ethanol was produced using 0.14 mL/L of  $\alpha$ -amylase enzyme [19]. Blending of alcohol in gasoline causes slight increases in NO<sub>x</sub> emissions but has led to the decrease in smoke and CO emissions [20]. Ethanol produced from fermented pomegranate fruit with 20% blending resulted in hydrocarbon emission of 65 ppm but raw petrol resulted in 150 ppm at engine load of 1500 rpm (Kirloskar, four stroke, single cylinder, spark engine) [21].

A variety of computational theoretical modeling approaches (artificial neural network (ANN), evolutionary computing and response surface methodology (RSM)) have recently been used for the optimization of bioprocesses [22]. RSM is one such empirical method that is valuable for designing, updating, and enhancing processes that are used to evaluate the impact of a variety of independent variables on the device output [23]. This method has been effectively utilized to optimize the alcoholic fermentation process [24, 25]. This modeling approach was used and tested for its suitability for the production of bioethanol process [26]. Until now, to the best of our knowledge, there was no study reported on bioethanol production from KR and SFW through fermentation using computational technique such as RSM.

The objective of the study was to utilize the processed algal waste present in the biofertilizer unit and food waste to produce an effective bioethanol as well as minimize

environmental pollution. Most of the studies used raw *Kappaphycus alvarezii* [27] and food waste [28] as raw materials for bioethanol production. To the best of our knowledge, for the first time, rejects of *Kappaphycus alvarezii* and food waste are currently being combined and used for bioethanol production. Furthermore, the purpose of this study was to optimize the experimental conditions such as inoculum size (vol%), pH, incubation time (h), and agitation speed (rpm) for maximum bioethanol production from KR and SFW. In addition, the bioethanol formation efficiency from reducing sugar was validated using logistic and modified Gompertz models. The produced bioethanol was analyzed using GC–FID and compared with standards.

## 2 Materials and method

### 2.1 Preparation of samples

The KR produced after sap (liquid) extraction was obtained from the Centre for Ocean research, Sathyabama Institute of Science and Technology, Tamil Nadu, Chennai, India. SFW was obtained from the mess hall of Sathyabama Institute of Science and Technology, Tamil Nadu, Chennai, India. Approximately 800 to 1000 kg of food waste was generated per day in the University mess. The samples collected were dried under sunlight in order to eliminate the water content of the samples and were powdered using a mixer grinder (Philips, HL7756/03, India) and sieved in 0.8 mm (SS200, Suntech Chennai) [29]. The prepared samples were stored in a zip lock cover and kept in a freezer (–5 °C). De ionized water (18.2 M $\Omega$ cm, Hindustan aqua system, Chennai) was used for performing all experiments in this study. All the chemicals used in these experiments were purchased from Sigma-Aldrich in analytical grade.

### 2.2 Biomass analysis

Moisture content (ASTM E949-88), ash content (ASTM E830-87), volatile matter (ASTM E897-88), and fixed carbon content were analyzed as per individual ASTM standards. The carbohydrate content of the KR, SFW, and KR:SFW (6:4 ratio) was determined using anthrone reagent method. In the anthrone reagent method, the samples were hydrolyzed under optimized conditions such as 2.5 N of phosphoric acid (H<sub>3</sub>PO<sub>4</sub>) hydrolysis at temperature of 80 °C for time of 3 h (from our previous study) [3].

### 2.3 Microorganism and growth conditions

Bread yeast (*Saccharomyces cerevisiae*) was purchased from local market (“Udaya” brand), Chennai, Tamil Nadu, India. At room temperature, the yeast was dispersed in distilled

**Table 1** Proximate analysis results of KR, SFW, and KR:SFW (6:4 ratio) with literature

Feedstock	Moisture content (wt%)	Ash content (wt%)	Fixed carbon (wt%)	Volatile matter (wt%)	References
KR	11.41	46	0.72	41.87	In this study
SFW	7.68	32.78	0.77	58.77	
KR:SFW (6:4)	9.13	17.05	2.97	70.85	
Green seaweed	8	19.6	13.1	59.3	[35]
Red seaweed	17.2	20.1	3.7	76.2	[2]
Brown seaweed	8	15.2	12	72.8	
Food wastes (mixed)	11.6	17	6.3	60.1	[34]
Food waste (white rice)	81.5	5.5	1.5	93	[36]

water at a concentration of 10 g/L. Initially, the yeast was incubated in agar plates comprising agar of 20 g/L, glucose of 20 g/L, peptone of 20 g/L, and yeast extract of 10 g/L for 48 h at 30 °C. A loop of yeast culture from the agar plate was transferred to Yeast Peptone Dextrose (YPD) medium and pre-cultivated for 24 h at 30 °C and 120 rpm in a shaking incubator [6].

### 2.4 Fermentation process

In our previous study, we optimized the *Kappaphycus alvarezii* reject and food waste at different proportions with different parameters such as (time, temperature, concentration, and duration) to obtain optimal yield. From this result, we chose the proportion KR:SFW (6:4 ratio) for the fermentation process [3]. Fermentation of KR, SFW, and KR:SFW (6:4 ratio) was performed in a 3-L fermenter (Merck, India). Pre-cultivated yeast inoculum of 10% (v/v) transferred to fermentation medium which comprises of diammonium sulfate (2 g/L), potassium hydrogen phosphate (1 g/L), potassium dihydrogen orthophosphate (1 g/L), zinc sulfate (0.2 g/L), magnesium sulfate (0.2 g/L), and yeast extract (2 g/L) respectively [30]. The prepared fermentation medium was sterilized using an autoclave at a temperature

of 121 °C for 20 min and cooled to room temperature. For the experiments, 10 g of KR, SFW, and KR:SFW (6:4 ratio) samples was hydrolyzed individually with 2.5 N (5.7 mL) of H3P04 at temperature of 80 °C for time of 3 h. The bioreactors loaded with the above-mentioned substrates had an overpressure of 1.2 bar during 30 min. Fermentation was carried out at various incubation time (24 to 60 h), pH from 4 to 6, agitation speed (60–120 rpm), and different inoculum sizes (3 to 15 vol%). The inoculation was accomplished aseptically condition and the inoculated hydrolysates were incubated for fermentation at 30 °C (± 1 °C). Immediately after inoculation, nitrogen gas was expelled into the bioreactors via the aeration device in order to achieve anaerobic conditions that were observed by the PO<sub>2</sub> electrode.

### 2.5 Fermentation kinetics

#### 2.5.1 Logistic model

The logistic model was used to evaluate the microbial kinetic parameters as per Eq. (1)

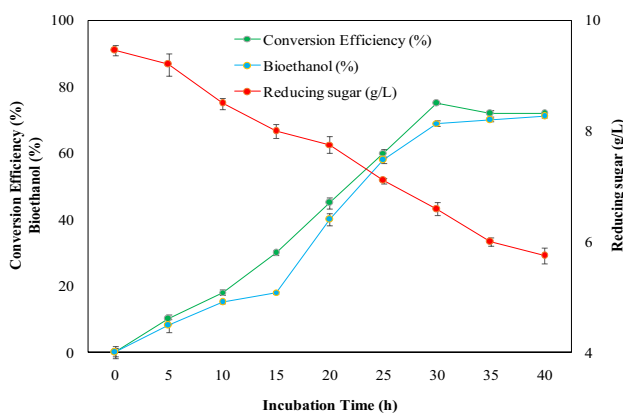


**Fig. 1** Effect of incubation time on bioethanol yield (%), reducing sugar concentration (g/L), and conversion efficiency (%) for KR

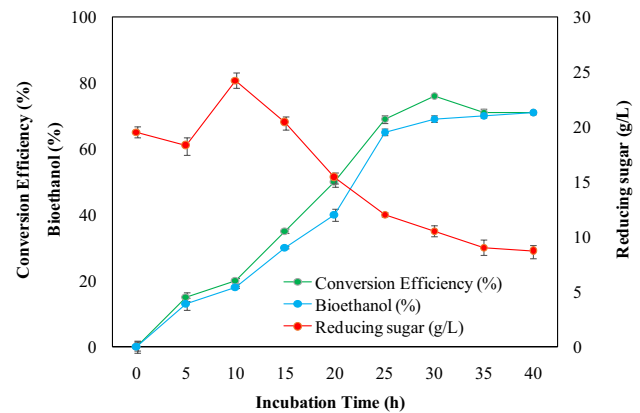


**Fig. 2** Effect of incubation time on bioethanol yield (%), reducing sugar concentration (g/L), and conversion efficiency (%) for SFW

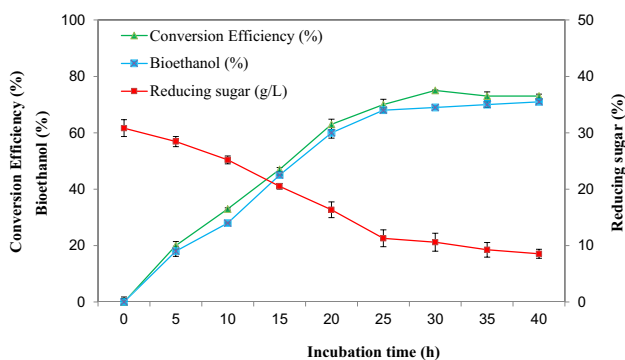


**Fig. 3** Effect of incubation time on bioethanol yield (%), reducing sugar concentration (g/L), and conversion efficiency (%) for KR:SFW

$$\ln(X/X_0) = \frac{\ln(X_{max}|X_0)}{\left\{ 1 + \exp\left[ \frac{4\mu_{max}}{\ln(X_{max}|X_0)}(\lambda - t) + 2 \right] \right\}} \quad (1)$$

where  $X_0$  denoted for initial biomass concentration (g/L),  $X_{max}$  for maximum biomass concentration (g/L),  $X$  for biomass concentration (g/L),  $t$  for incubation time (h),  $C_{pmax}$  for maximum specific growth rate ( $h^{-1}$ ), and lag time (h) respectively [26].

**2.5.2 Modified Gompertz model**

The experimental observation of bioethanol concentration vs time was fitted in to modified Gompertz model as per Eq. (2).

$$C_p = C_{pmax} \times \exp\left\{ -\exp\left[ K_{Pmax} \times \exp(1)/C_{pmax} \right] \times (tL - t) + 1 \right\} \quad (2)$$

From the equation,  $C_p$  is denoted for bioethanol concentration (g/L),  $C_{pmax}$  is maximum bioethanol concentration (g/L),  $K_{Pmax}$  is maximum production rate (g/L/h), and  $tL$  is represented as time from the beginning of the fermentation

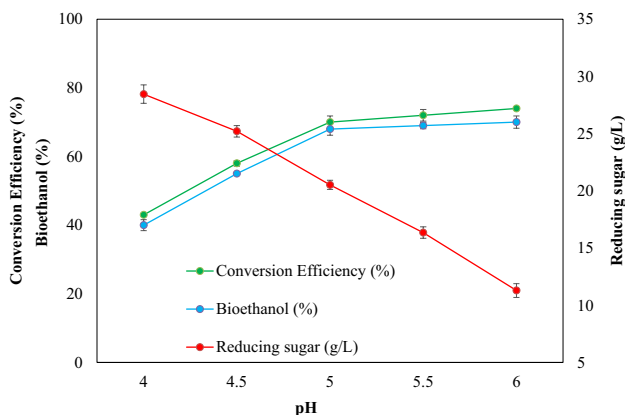


**Fig. 4** Effect of pH on bioethanol yield (%), reducing sugar concentration (g/L), and conversion efficiency (%) for KR

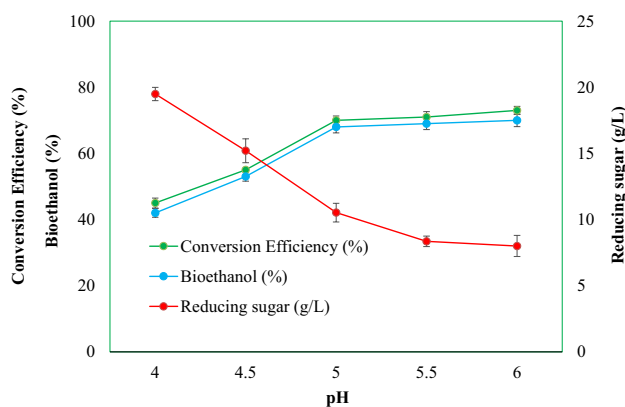


**Fig. 5** Effect of pH on bioethanol yield (%), reducing sugar concentration (g/L), and conversion efficiency (%) for SFW

to exponential bioethanol production (h) [31]. These kinetic parameters were predicted from the non-linear regression using MATLAB software (Version 19, Mathworks; Natick, MA).

**2.6 Response surface methodology**

The RSM technique was used to determine modeling and optimization of bioethanol production. Central composite design (CCD) at three levels was employed for designing the experimental data [30]. Design-Expert version 7.0 was used to quantify the results of the variables and their correlations. To evaluate the potential of ethanol yield from KR:SFW, 30 experiments (16 factorial, 8 axial, and 6 centers) were conducted according to the CCD method. The evaluation of variables and their regressions was also conducted to assess the significance of the model. The four independent variables such as (a) inoculum size (vol%), (b) pH, (c) incubation time (h), and (d) agitation speed (rpm) were considered as input parameters and the bioethanol yield (%) considered as output of the RSM. The levels of different coded parameters are (1) inoculum size (A) range between 3 and 15 vol%;

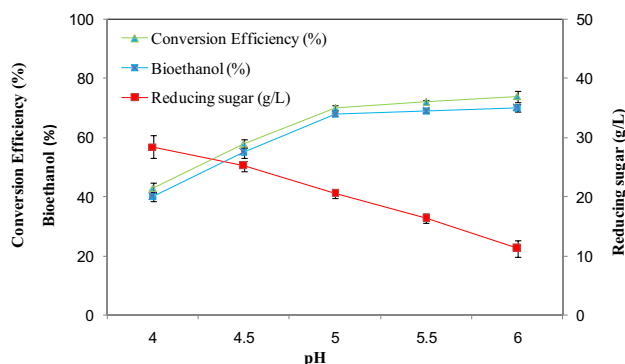


**Fig. 6** Effect of pH on bioethanol yield (%), reducing sugar concentration (g/L), and conversion efficiency (%) for KR:SFW

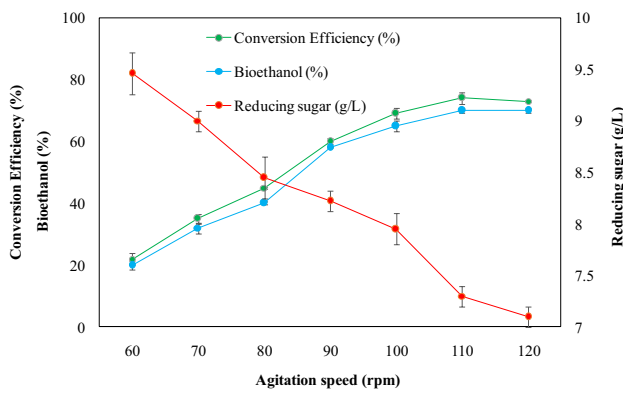


**Fig. 7** Effect of agitation speed on bioethanol yield (%), reducing sugar concentration (g/L), and conversion efficiency (%) for KR

(2) pH (*B*) range between 4 and 6; (3) incubation time (*C*) range between 24 and 60 h; and (4) agitation speed (*D*) range between 60 and 120 rpm [32].

### 2.7 GC FID analysis

The presence of bioethanol in the samples was examined using a gas chromatography YL 6500 (Spain) system joined with a Hewlett Packard device equipped with the YL-Clarity software. A flame ionization detector (FID) is equipped for gas chromatography [33]. The length of the capillary column was 30 m, the diameter was 0.53 mm, and the thickness of the capillary column is 1 μm. It is packed with polyethylene glycol. Helium is used as a carrier gas at a steady flow rate of 3 mL/min. The ignition and maximum temperature for FID were set to 471 K and 513 K respectively. The injection volume of 1 μL and a split ratio of 10:1 were used as part of the GC–FID analysis. The run time of the samples was 30 min. After analysis of the samples, the oven was cooled to 323 K for further analysis.

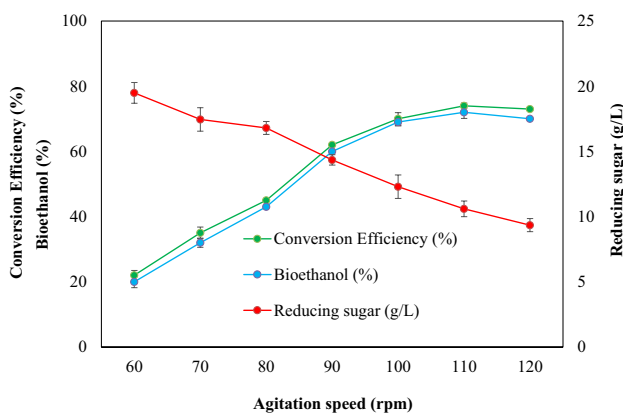


**Fig. 8** Effect of agitation speed on bioethanol yield (%), reducing sugar concentration (g/L), and conversion efficiency (%) for SFW

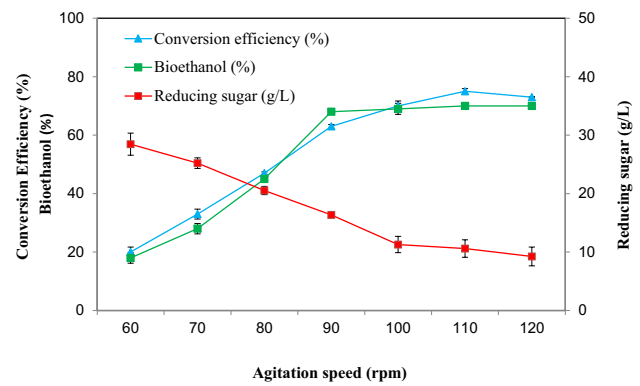


**Fig. 9** Effect of agitation speed on bioethanol yield (%), reducing sugar concentration (g/L), and conversion efficiency (%) for KR:SFW

## 3 Results and discussion

### 3.1 Biomass characterization

The proximate analysis was preferred to determine the essential fractions of biomass like moisture content, ash content, volatile matter, and fixed carbon. The moisture content in the biomass was an important factor for determining the bioethanol yield. Moisture content of KR, SFW, and KR:SFW was 11.41 wt%, 7.68 wt%, and 9.13 wt%. It was stated that lesser the moisture, higher the bioethanol yield [3]. The proximate analysis of KR, SFW, and KR:SFW is shown in Table 1. The ash content of biomass also plays an important role in bioethanol formation. The ash content of KR was 46 wt%, SFW was 58.77 wt%, and KR:SFW was 17.05 wt% respectively. In another study, *Gracilaria corticata var corticata* algae had an ash content of 20.1 wt (%) [2]. The volatile matter of KR, SFW, and KR:SFW were 41.87 wt%, 58.77 wt%, and 70.85 wt% respectively. In another study with food waste (white rice) had volatile

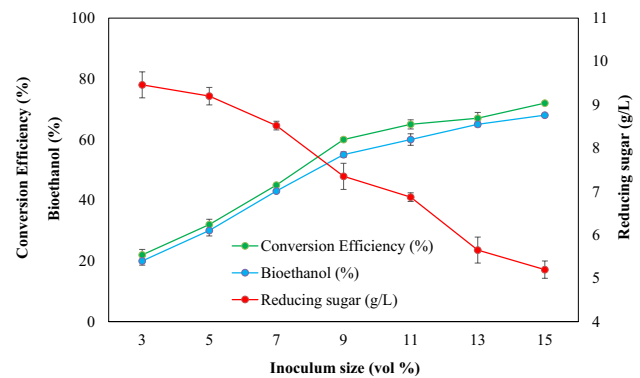


**Fig. 10** Effect of inoculum size on bioethanol yield (%), reducing sugar concentration (g/L), and conversion efficiency (%) for KR



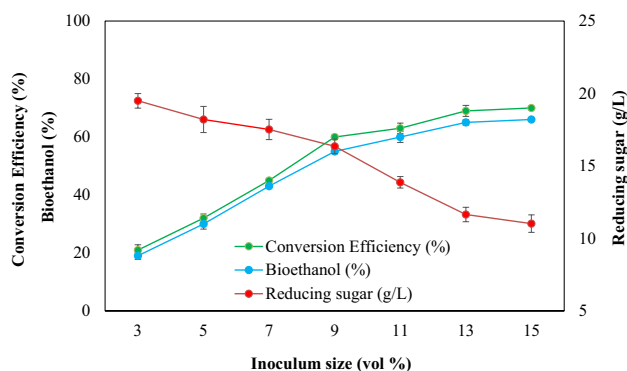


**Fig. 11** Effect of inoculum size on bioethanol yield (%), reducing sugar concentration (g/L), and conversion efficiency (%) for SFW

matter of 60.1 wt% [34]. Mainly, the KR:SFW was rich in reducing sugar concentration and it can be used as an alternative biomass for bioethanol production through the fermentation process.

## 3.2 Fermentation studies

### 3.2.1 Effect of incubation time on bioethanol yield

Fermentation of KR, SFW, and KR:SFW was carried out at various incubation times (24 to 60 h), pH of 5, agitation speed of 90 rpm, and different inoculum sizes of 15 vol%. Figures 1, 2, and 3 show the relationship between the reducing sugar concentration (g/L), conversion efficiency (%), and bioethanol yield (%) against incubation time at lab scale. Figure 3 (KR:SFW) shows the Maximum bioethanol yield was 68% at 25 h of incubation time. At an incubation time of 25 h, the reducing sugar concentration was reduced to 11.29 g/L from 30.83 g/L with a conversion efficiency of 70%. For KR, maximum bioethanol yield was 58% (Fig. 2) and SFW was 65% (Fig. 3) with maximum conversion efficiency of 60% and 69%. From the findings, it was clear that

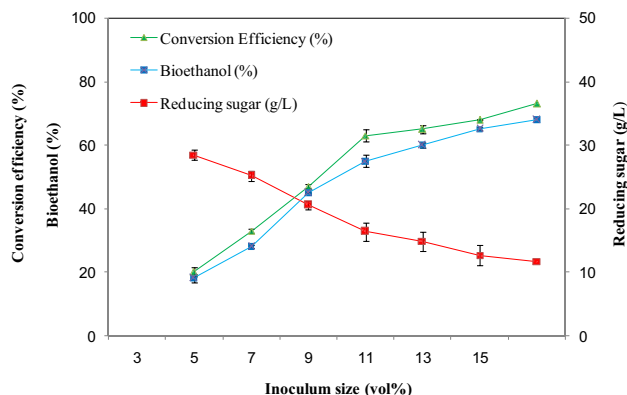


**Fig. 12** Effect of inoculum size on bioethanol yield (%), reducing sugar concentration (g/L), and conversion efficiency (%) for KR:SFW

the increase in the concentration of bioethanol indicates the considerable consumption of reducing sugars by *Saccharomyces cerevisiae* yeast during that fermentation time. Similar results were obtained from Asmamaw Tesfaw et al.'s studies; increasing the reducing sugar content derived from food waste leachate from 45 to 75 g/L enhanced ethanol production by 2.3-fold using *S. cerevisiae* KCTC-7904 [37].

### 3.2.2 Effect of pH on bioethanol yield

The pH plays an important role during fermentation because all the organism and cellular processes are affected by pH, that is, because of H<sup>+</sup> ion concentration in the liquid medium. pH 5 was suitable for cell growth because the high acidic or basic condition of the medium affects the metabolic activities of yeast and cell growth [38]. Figures 4, 5, and 6 indicate the reducing sugar concentration (g/L), conversion efficiency (%), and bioethanol yield (%) against pH at the lab scale. In our present study, the experiment is conducted at pH 4 to 6. From the results, pH 5 resulted in higher bioethanol yield (68%) than pH 4 (40%) after 24 h of fermentation time. At pH 5, reducing sugar concentration was 20.52 (g/L) with conversion efficiency of 70% for KR:SFW (Fig. 6). Moreover, KR shows reducing sugar concentration was 4.52 (g/L) with a conversion efficiency of 60% and SFW shows reducing sugar concentration was 10.52 (g/L) with a conversion efficiency of 70%. It was clearly indicated that KR:SFW gave high yield compared to KR and SFW.

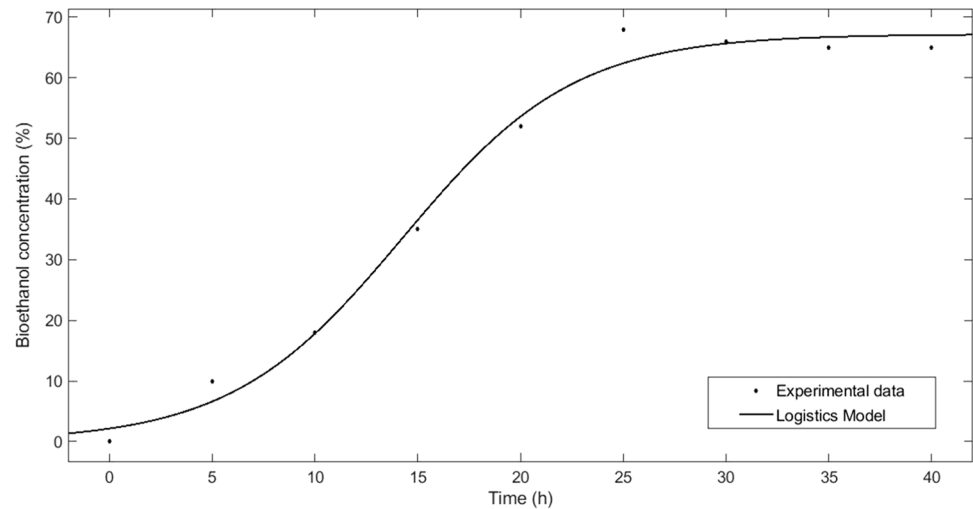
### 3.2.3 Effect of agitation speed on bioethanol yield

The role of reducing sugar concentration (g/L), conversion efficiency (%), and bioethanol yield (%) against agitation speed (60, 70, 80, 90, 100, 110, and 120 rpm) is shown in Figs. 7, 8, and 9. Lower the agitation time, higher the bioethanol formation [39]. From the results, KR:SFW (Fig. 9) shows at 90 rpm, reducing sugar concentration reduced to 16.35 g/L from 30.83 g/L with the conversion efficiency of 63%, which is higher than KR (Fig. 7) and SFW (Fig. 8). The maximum ethanol yield was 68% at an incubation time of 24 h of 90 rpm obtained from KR:SFW (Fig. 9). Oxygen plays an important role during the fermentation process. Excessive oxygen in the fermentation medium will lead to enhanced cell growth [40].

### 3.2.4 Effect of inoculum size on bioethanol yield

Figures 10, 11, and 12 provide information regarding reducing sugar concentration (g/L), conversion efficiency (%), and bioethanol yield (%) against varying inoculum size concentration (3 to 15 vol%). From Figs. 10, 11, and 12, it was seen that inoculum size was directly

**Fig. 13** Fitting of the logistic to the experimental results of bioethanol concentration (g/L) vs time (h)



proportional to the bioethanol production. Higher the inoculum size comprises more number of yeast cells which in turn results in higher reducing sugar consumption and this results in higher conversion percentage [41]. Figure 12 shows the bioethanol yield and reducing sugar concentration of KR: SFW. From the results, it is evident that the reducing sugar concentration reduced to 11.67 g/L with the conversion efficiency of 73% respectively.

### 3.3 Fermentation kinetics

Logistic and modified Gompertz models are used to determine the kinetic parameters of the fermentation process (Figs. 13 and 14). The experimental results for these kinetic parameters are represented in Table 2. The methodological findings have indicated that the two models are quite well calibrated for experimental data ( $R^2$  and RMSE) and also the overall rate of specific growth ( $\mu_{max}$ ) was the key parameter that has an effect on the concentration of bioethanol.

Thus, accurately estimating the  $\mu_{max}$  value was important for enhancing the bioethanol production [42]. N. Phukoetphim et al. reported biomass such as sweet sorghum juice produced bioethanol (0.49 g/g) using a modified Gompertz kinetic model [43].

Gompertz's modified model incorporated fermentation kinetics findings are denoted in Table 2. Maximum bioethanol concentration ( $C_{pmax}$ ), maximum production rate ( $K_{Pmax}$ ), and the latency period ( $tL$ ) were analyzed. The observations revealed a high significant relation between the experimental results and the model ( $R^2=0.98$ ). In this experiment, the high percentage of bioethanol concentration yield was 4.016 g/L, which is comparable to bioethanol produced from potato peel waste (5.30 g/L) [44]. On the other hand, maximum bioethanol production through the modified Gompertz model was 69.07 g/L. The earliest stage was represented as the lag phase of the growth cycle. In the present study, the lag phase occurred in the duration of 9 h, which is less than found in 12 h [45]. It was stated that the lag phase

**Fig. 14** Fitting of the modified Gompertz models to the experimental results of bioethanol concentration (g/L) vs time (h)

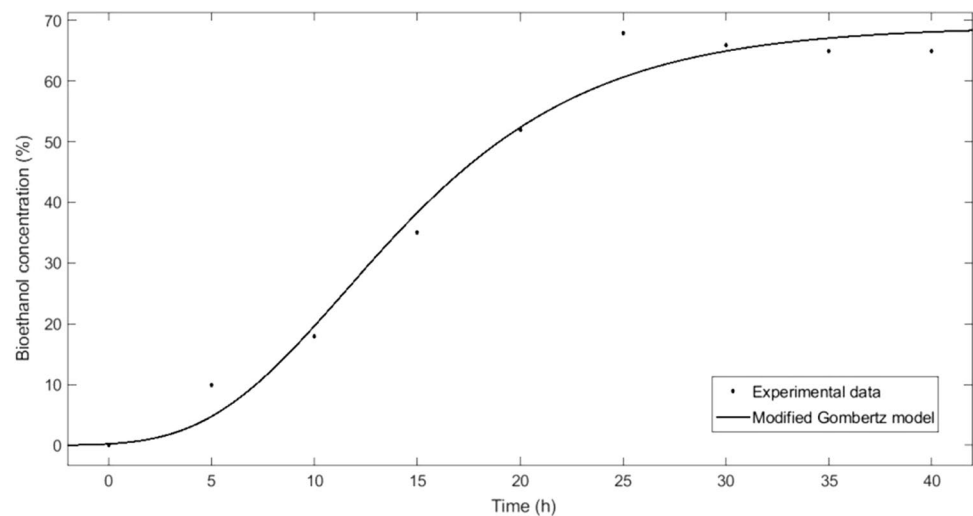


**Table 2** Kinetic parameters of fermentation of KR:SFW using logistic and modified Gompertz models

Model	Logistic	Modified Gombertz
Kinetic parameters	$\ln(X_{max} X_0) = 67.19$ $\mu_{max} = 4.016$ $\lambda = 5.902$	$K_{pmax} = 69.07$ $C_{pmax} = 3.871$ $tL = 4.899$
$R^2$	0.9898	0.981
RMSE	3.154	4.297

was directly proportional to the substrate composition and process of bioethanol production [46].

### 3.4 RSM statistical analysis

The obtained RSM experimental data was fitted to four types of models such as linear, two-factor interaction (2FI), quadratic, and cubic polynomials. Based on Table 3, it is concluded that the quadratic model is the best model for representing the relationship between the factors and response. The cubic model could not be used for further modeling of the experimental data because the model was found to be aliased. Aliased model occurs due to lack of experimental run to independently estimate all the terms for that model [32, 47]. The second highest order polynomial model with insignificant lack-of-fit must be the choice and hence the quadratic model was selected. A good model should have a low standard deviation (SD); high coefficient of determination  $R$ -squared ( $R^2$ ) (raw, adjusted, and predicted); and low PRESS (predicted residual sum of squares) [32, 48]. Based on Table 3, quadratic model is the best model to describe the relationship of the factors to the response, since it has the lowest SD; highest  $R^2$  (raw, adjusted, and predicted); and lowest PRESS. It can be concluded that the quadratic model is the best polynomial model to describe the relationship between the independent variables and their response.

Based on Table 4, the model  $F$ -value of 194.24 implies the model is significant. There is only a 0.01% chance that an  $F$ -value this large could occur due to noise.  $P$ -values less than 0.05 indicate model terms are significant. In this case,  $A, B, D, AB, AC, BD, CD, AA^2, BA^2, CA^2,$  and  $DA^2$  are significant model terms. Values greater than 0.1 indicate the model terms are not significant. If there are many insignificant model terms (not counting those required to support

hierarchy), model reduction may improve the model. The lack of fit  $F$ -value of 1.24 implies the lack of fit is not significant relative to the pure error (Table 5). There is a 43.05% chance that a lack of fit  $F$ -value this large could occur due to noise. The predicted  $R^2$  of 0.97 is in reasonable agreement with the adjusted of  $R^2$  0.98. Adeq precision measures the signal to noise ratio. A ratio greater than 4 is desirable. Ratio of 45.986 indicates an adequate signal. This model can be used to navigate the design space. The coefficient estimate represents the expected change in response per unit change in factor value when all remaining factors are held constant. The intercept in an orthogonal design is the overall average response of all the runs [49].

Based on Table 4,  $A, B, D, AB, AC, BD, CD, AA^2, BA^2, CA^2,$  and  $DA^2$  are significant model terms. The predicted output of the model was considered to be significant with  $R^2$  of 0.9752. The predicted and adjusted  $R^2$  values were 0.9894 and were considered to be in fair agreement, i.e., the difference is less than 0.2. The quadratic regression model bioethanol yield of bioethanol fermentation from KR:SFW residues by *S. cerevisiae* obtained from CCD in terms of actual factors is presented in Eq. (3).

$$\begin{aligned}
 \text{Bioethanol yield} = & -1.746 + 0.058(\text{Inoculum size}) \\
 & + 0.664(\text{pH}) + 0.0079(\text{Incubation time}) \\
 & + 0.00286(\text{rpm}) - 0.00062(\text{Inoculum size})(\text{pH}) \\
 & - 0.0010(\text{inoculum size})(\text{Incubation time}) \\
 & + 2.31E - 05(\text{Inoculum size})(\text{agitation speed}) \\
 & - 0.0001(\text{pH})(\text{incubation time}) - 0.001(\text{pH}) \\
 & (\text{agitation speed}) - 3.82E - 05(\text{incubation time}) \\
 & (\text{agitation speed}) - 0.0001 \text{Inoculum size}^2 \\
 & - 0.063\text{pH}^2 + 8.20E - 05 \text{incubation time}^2 \\
 & + 1.98E - 05 \text{agitation speed}^2
 \end{aligned}
 \tag{3}$$

The equation in terms of actual factors can be used to make predictions about the response to given levels of each factor. Here, the levels should be specific in the original units for each factor. This equation should not be used to determine the relative impact of each factor because the coefficients are scaled to accommodate the units of each factor and the intercept is not at the center of the design space. From Eq. 3, the positive symbol represents synergistic effect in the

**Table 3** Summary of probability values and model summary statistics

Source	Standard deviation	Adjusted $R$ -squared	Predicted $R$ -squared	$R$ -squared	PRESS	
Linear	0.1162	0.2199	0.0951	-0.2055	0.5219	
2FI	0.1008	0.5538	0.3191	0.2963	0.3046	
Quadratic	0.0125	0.9945	0.9894	0.9752	0.0107	Suggested
Cubic	0.0116	0.9978	0.9910	0.9118	0.0382	Aliased



**Table 4** Experimental design data

S. No	Standard	Run	Space type	A	B	C	D	Bioethanol yield (% w/w)	Theoretical bioethanol yield (%w/w)
1	6	3	Factorial	15	4	60	60	0.44	0.46
2	15	4	Factorial	6	6	60	120	0.39	0.40
3	3	5	Factorial	6	6	24	60	0.34	0.36
4	1	6	Factorial	6	4	24	60	0.35	0.37
5	8	9	Factorial	15	6	60	60	0.55	0.58
6	11	10	Factorial	6	6	24	120	0.29	0.31
7	14	12	Factorial	15	4	60	120	0.45	0.46
8	16	15	Factorial	15	6	60	120	0.41	0.44
9	7	17	Factorial	6	6	60	60	0.52	0.53
10	12	18	Factorial	15	6	24	120	0.62	0.64
11	13	20	Factorial	6	4	60	120	0.54	0.56
12	10	22	Factorial	15	4	24	120	0.67	0.69
13	4	23	Factorial	15	5	24	90	0.68	0.70
14	5	26	Factorial	6	4	60	60	0.56	0.57
15	2	28	Factorial	15	4	24	60	0.57	0.59
16	9	30	Factorial	6	4	24	120	0.41	0.43
17	24	1	Axial	10.5	5	42	150	0.58	0.60
18	20	2	Axial	10.5	7	42	90	0.26	0.28
19	19	7	Axial	10.5	3	42	90	0.3	0.32
20	17	11	Axial	1.5	5	42	90	0.28	0.30
21	18	13	Axial	19.5	5	42	90	0.51	0.53
22	21	19	Axial	10.5	5	6	90	0.63	0.65
23	23	25	Axial	10.5	5	42	90	0.63	0.65
24	22	29	Axial	10.5	5	78	90	0.65	0.67
25	29	8	Center	10.5	5	42	90	0.53	0.56
26	26	14	Center	10.5	5	42	90	0.54	0.56
27	25	16	Center	10.5	5	42	90	0.54	0.55
28	30	21	Center	10.5	5	42	90	0.53	0.54
29	28	24	Center	10.5	5	42	90	0.53	0.55
30	27	27	Center	10.5	5	42	90	0.56	0.58

highest bioethanol yield, whereas negative sign represents antagonistic effect [49].

### 3.5 Validation of RSM

The main part of the experiment was to predict the suitability of the developed model. The interaction between the predicted and actual bioethanol yield values is shown in Fig. 15. It was seen that there was a positive correlation ( $R^2 = 0.989$ ) between the predicted and the experimental values, representing that the predicted and the experimentally obtained values are in good agreement. This implies that the results match well with the model and give a convincingly strong approximation for the system in the experimental range examined. Figure 16 displays the normal probability plots of the standardized residues for bioethanol production effectiveness.

A normal probability plot shows that if the residuals obey a normal distribution, then the points should form a straight line. Since some refraction is anticipated even for normal data, as seen in Fig. 16, it can be concluded that the data is distributed normally. Thus, the normal probability plot suggests strong validity for the estimate of the quadratic regression model. Figure 17 displays residual vs. expected bioethanol yield values. In this analysis, the points of the observed runs were randomly dispersed across the constant residual range throughout the line. As a result, there was no clear pattern and peculiar structure. That is, the model is sufficient and there is no reason to assume any deviation of the independence or a continuous deviation in all cases. The standardized residual against run plot displayed in Fig. 18 shows arbitrarily dispersed points; the errors were distributed normally and are negligible [50].

**Table 5** Analysis of variances (ANOVA) for the quadratic model

Source	Sum of squares	Degrees of freedom	Mean square	F-value	p-value	
Model	0.4305	14	0.0307	194.24	2.46E-14	Significant
A	0.0876	1	0.0876	553.28	2.97E-13	
B	0.0030	1	0.0030	19.18	0.0005	
C	3.75E-05	1	3.75E-05	0.23	0.6335	
D	0.0045	1	0.0045	28.65	8.05E-05	
AB	0.0126	1	0.0126	79.93	2.13E-07	
AC	0.1072	1	0.1072	677.40	6.74E-14	
AD	0.0001	1	0.0001	0.98	0.3362	
BC	0.0001	1	0.0001	0.98	0.3362	
BD	0.0175	1	0.0175	110.88	2.52E-08	
CD	0.0068	1	0.0068	42.98	9.10E-06	
AA <sup>2</sup>	0.0330	1	0.0330	208.43	3.33E-10	
BA <sup>2</sup>	0.1103	1	0.1103	697.14	5.46E-14	
CA <sup>2</sup>	0.0193	1	0.0193	122.22	1.31E-08	
DA <sup>2</sup>	0.0087	1	0.0087	54.96	2.17E-06	
Residual	0.0023	15	0.0001			
Lack of fit	0.0016	10	0.0001	1.23	0.430472	Not significant
Pure error	0.0006	5	0.0001	194.24		
Total	0.4329	29		553.28		

### 3.6 Optimum conditions and effect of process variables

Numerical optimization was implemented to obtain the optimal conditions. The highest potential bioethanol yield

was observed when the process conditions were at inoculum size of 15 vol%, initial pH 5, 24 h of incubation period (h), and 90 agitation speed (rpm). The expected yield of the bioethanol from suggested fermentation condition was 0.70% (w/w). Selectively, four interaction terms between

**Fig. 15** Experimental values vs predicted values for the model

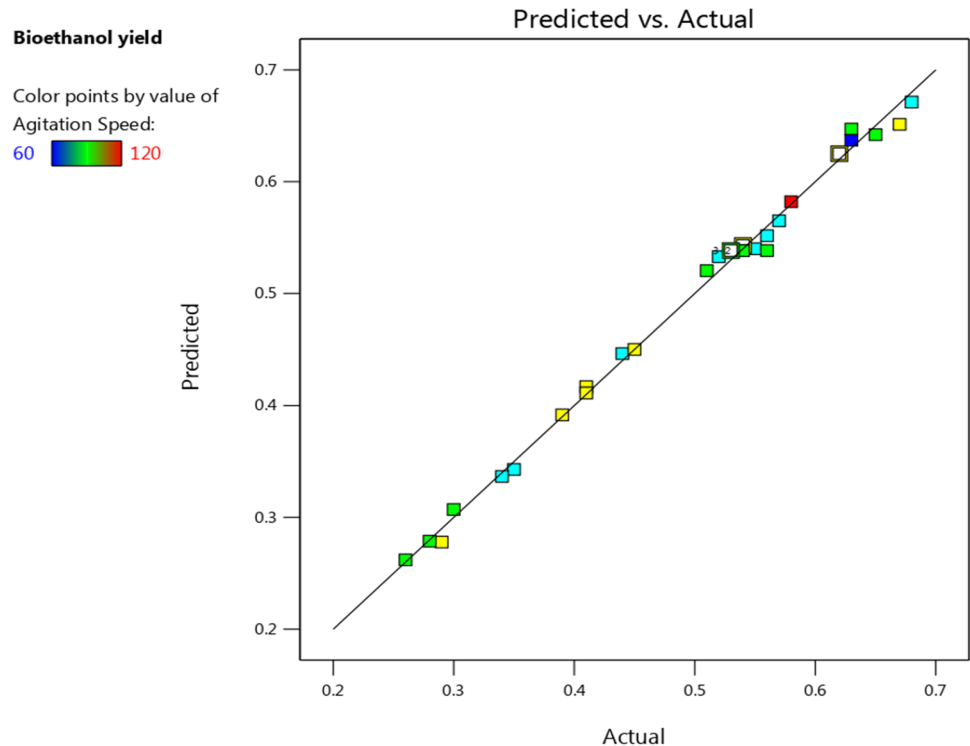
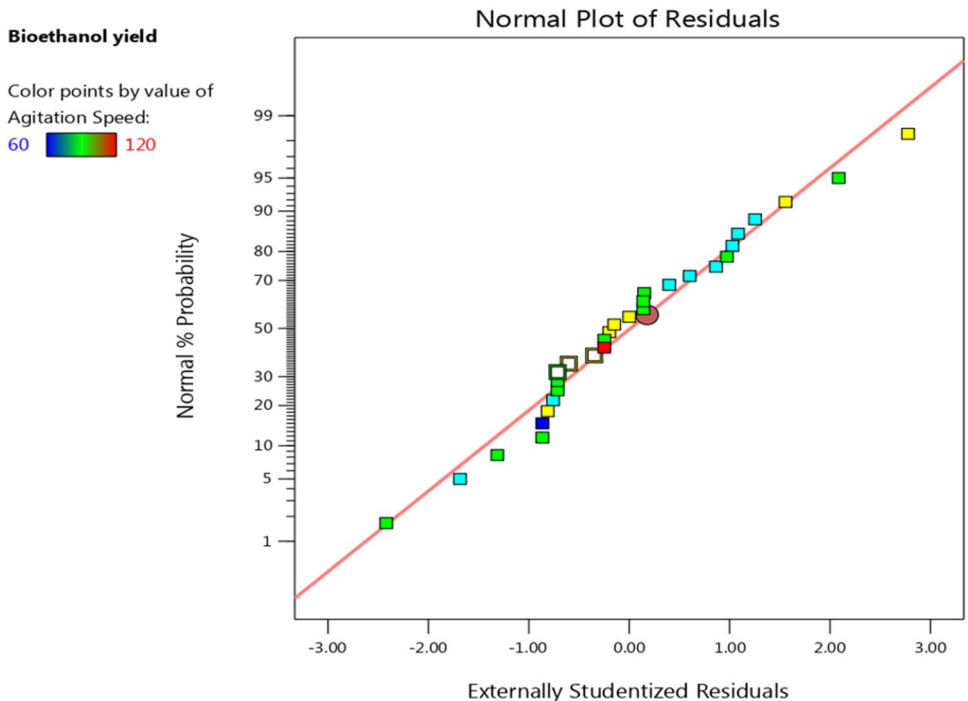


**Fig. 16** Normal probability plot of the residuals



the factors had a major impact on the yield of bioethanol during fermentation which is obtained from ANOVA test. They were coded as *AB*, *AC*, *BD*, and *CD*, which represented the interaction between the inoculum size (mL) and pH, the inoculum size (mL) and incubation time (h),


pH and agitation speed (rpm), and incubation time (h) and agitation speed (rpm). The contour plots of interaction between inoculum size (vol%), pH, incubation time (h), and agitation speed (rpm) are represented in Fig. 19, Fig. 20, Fig. 21, and Fig. 22.

**Fig. 17** Diagnostic plots for bioethanol yield residual vs predicted yield

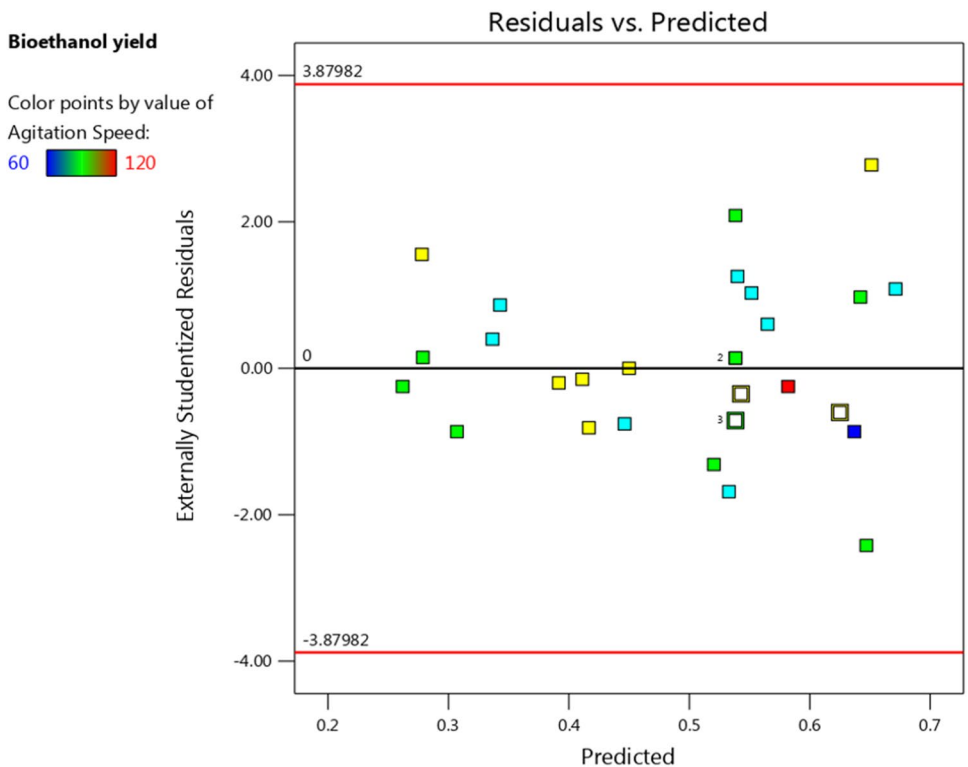


**Fig. 18** Diagnostic plots for bioethanol yield residual vs run number

**Bioethanol yield**

Color points by value of Agitation Speed:  
60  120

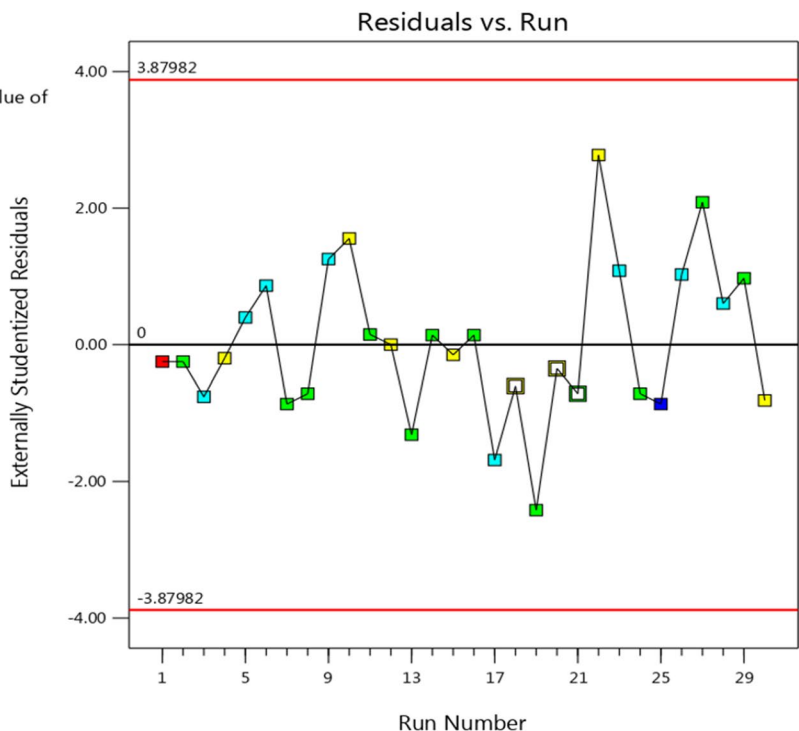


**Fig. 19** Contour plot for inoculum size (vol%) and incubation time (h)

Factor Coding: Actual

**Bioethanol yield (% w/w)**

0.26  0.68

X1 = A

X2 = C

**Actual Factors**

B = 5.06

D = 90

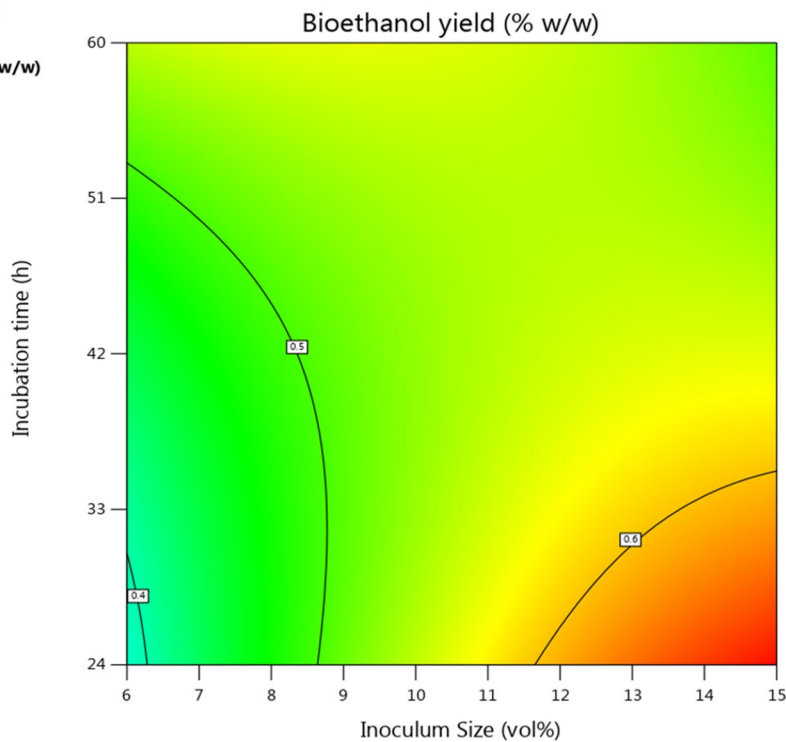


**Fig. 20** Contour plot for pH and inoculum size (vol%)

Factor Coding: Actual

**Bioethanol yield (% w/w)**

● Design Points

0.26 0.68

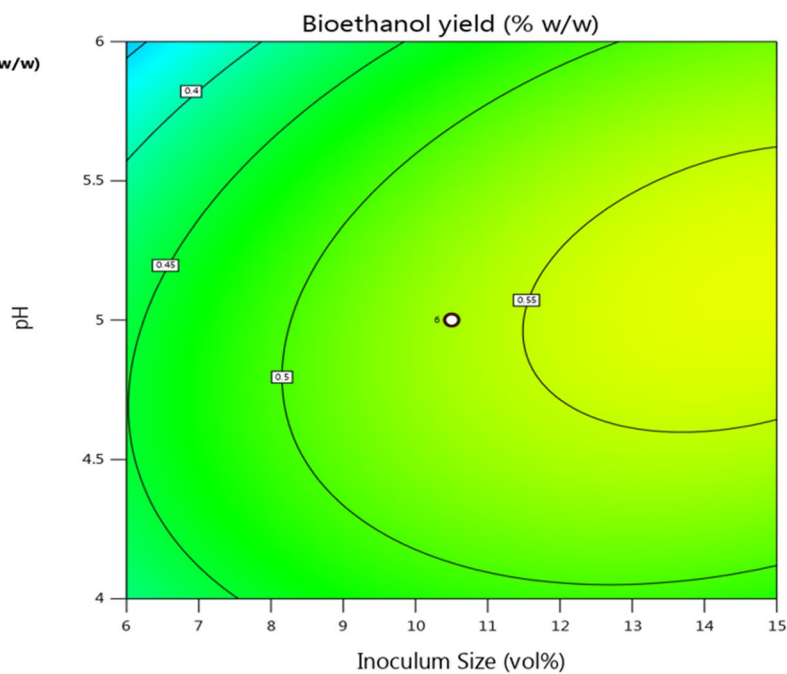
X1 = A

X2 = B

**Actual Factors**

C = 42

D = 90



The figures show the interaction between respective parameters, optimum conditions, and their yield. The contour plot of interaction between incubation time and inoculum size displayed a part of an ellipses pattern. An elliptical contour plot means that the center of the plot showed a maximum response as described by Bas et al. [51]. The obtained bioethanol percentage was higher than bioethanol recovered from palm trunk biomass (0.45 g/g) and their effluent [32].

### 3.7 Optimization of bioethanol production using response surface methodology

The 3D plot of Fig. 23 explains the relationship between pH (range of 4 to 6) and inoculum size (3 to 15 vol%) to KR:SFW at a stable incubation time (42 h) and 90 agitation speed to bioethanol yield. The bioethanol yield of 0.56% (w/w) was obtained and a steady rise in the bioethanol yield percentage was established. The gradual decline

**Fig. 21** Contour plot for agitation speed (rpm) and incubation time (h)

Factor Coding: Actual

**Bioethanol yield (% w/w)**

0.26 0.68

X1 = C

X2 = D

**Actual Factors**

A = 10.5

B = 5.06

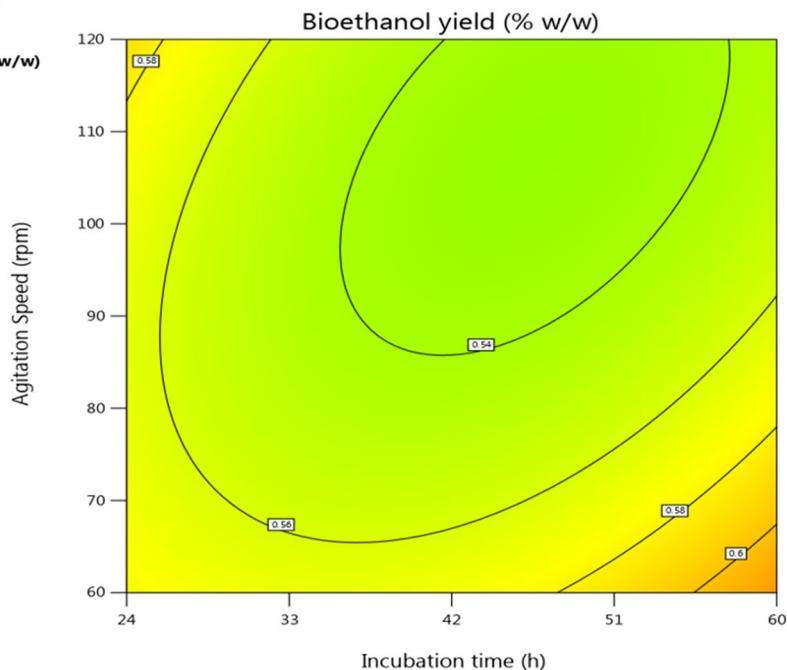
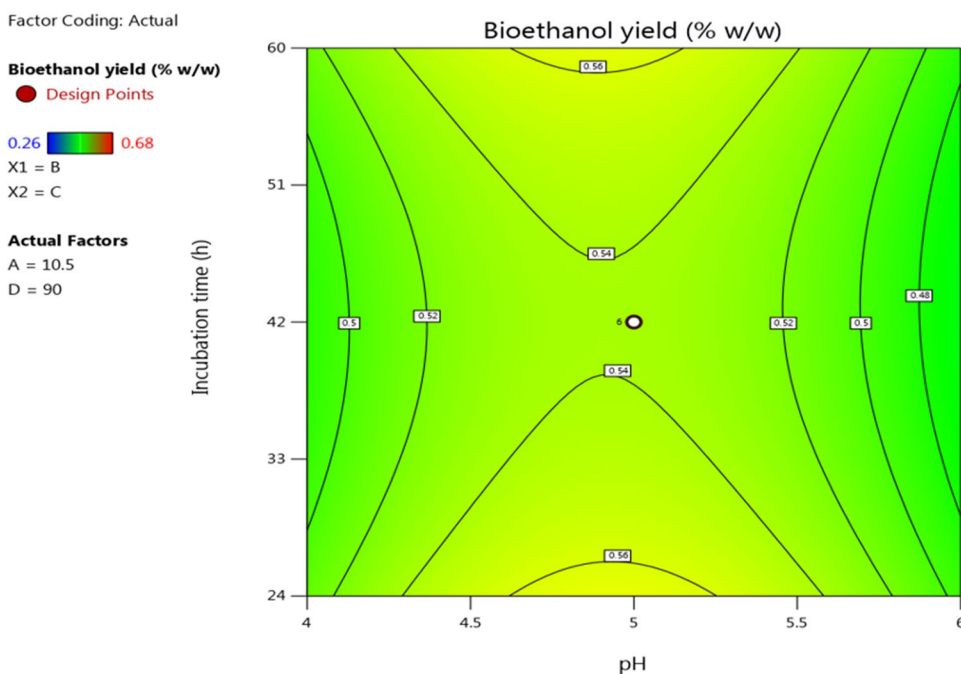




**Fig. 22** Contour plot for pH and incubation time (h)



in the bioethanol yield percentage resulted owing to an increase in incubation period and agitation speed. Figure 24 describes the influence of incubation time (range of 24 to 60 h) and inoculum size (3 to 15 vol%) at constant pH (5) and agitation speed (90 rpm). The 3D plot reveals that the bioethanol yield obtained ranges from 0.53% (w/w) to 0.68% (w/w). The maximum bioethanol from plot

is 0.68% (w/w). Figure 25 represents the effect of agitation speed (60 to 120 rpm) and inoculum size (3 to 15 vol%) at a constant pH (5) and incubation time (42 h). Figure 26 reflects the incubation time between 24 and 60 h and pH of 4–6 at a stable inoculum size of 10.5 mL. From the results, at 42 h of incubation time indicated a significant drop in bioethanol yield from 0.51% (w/w) to 0.49% (w/w). Thus,

**Fig. 23** 3D plots for pH and inoculum size

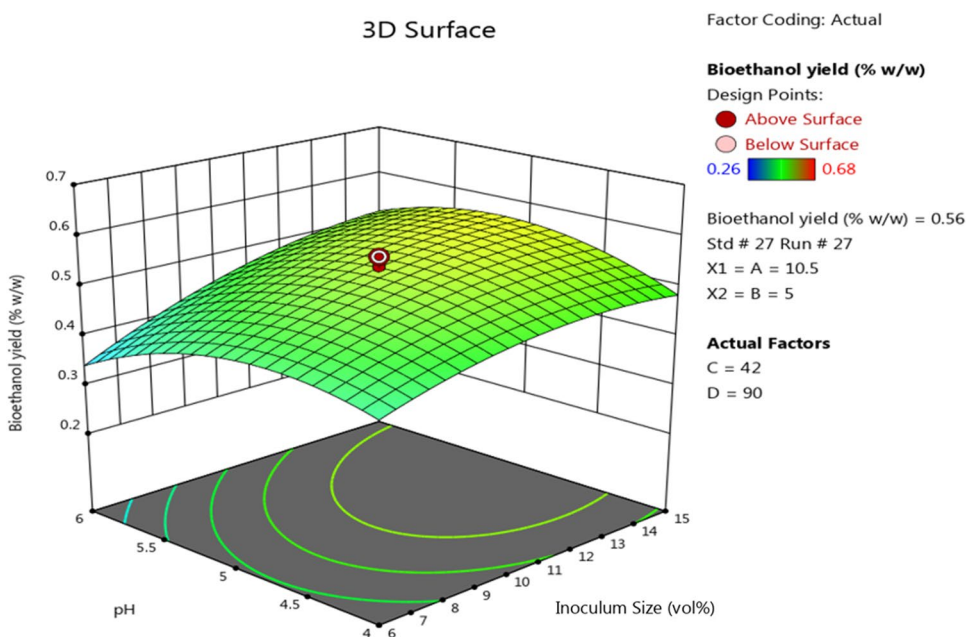
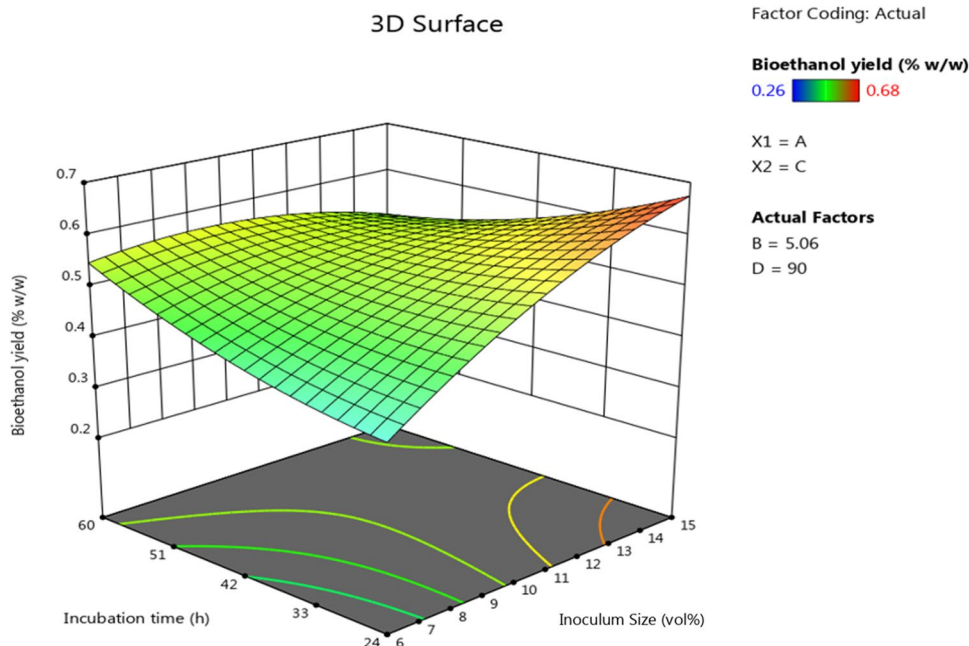


**Fig. 24** 3D plots for incubation time and inoculum size



24 h of incubation period for KR:SFW, 15 (vol%) inoculum size, pH5, and 90 agitation speed (rpm) are inferred to be the optimum conditions required to achieve 0.68% (w/w) of the bioethanol yield.

### 3.8 GC analysis

Fermented samples were collected and distilled using a rotary evaporator (SA-RE29T43, SPAN) at 80 °C, 100 rpm

for 30 min. The distilled samples were subjected to gas chromatography (YL 6500GC) flame ionization detector (FID). For confirmation, chemical grade ethanol was injected as standard to GC FID (Fig. 27). The obtained peak was compared with KR:SFW bioethanol peak (Fig. 28). The peaks show the following components in negligible amount present in the bioethanol sample: retention time (2.92) — isopropanol, retention time (2.97) — isoflurane, retention time (3.9) — bioethanol, retention time (6.4) — toluene, retention

**Fig. 25** 3D plots for agitation speed and inoculum size

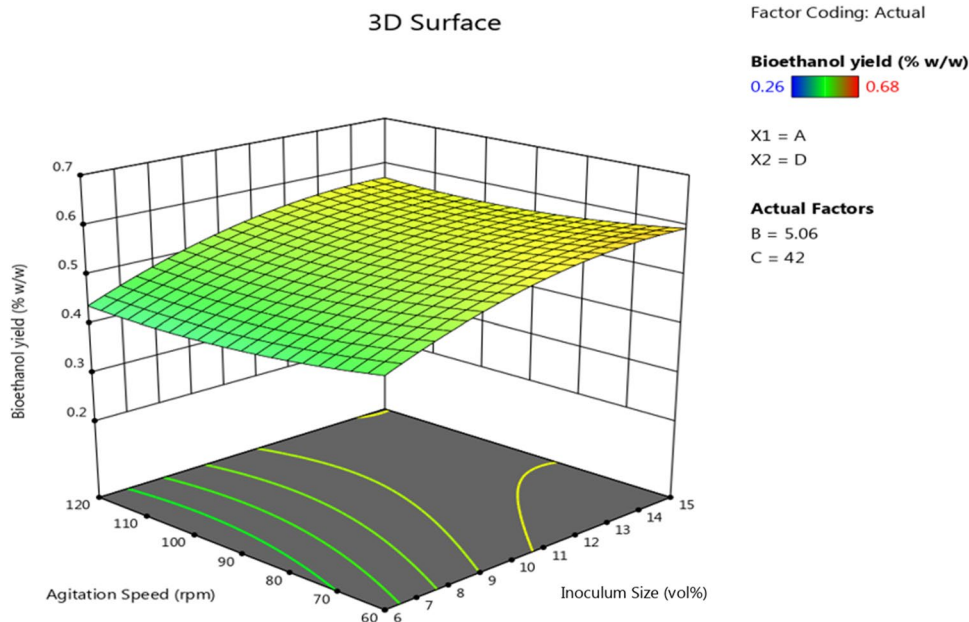
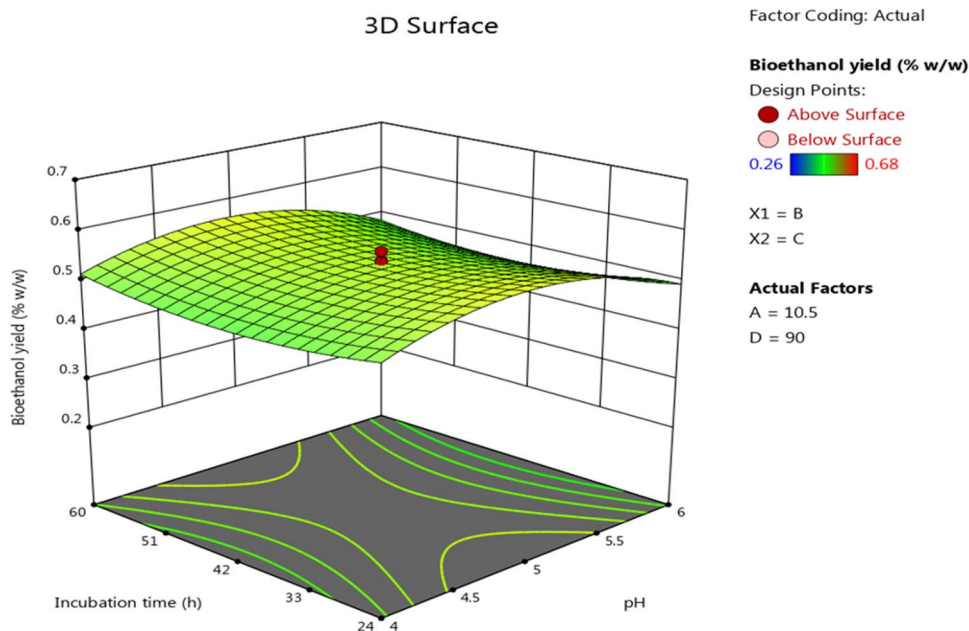


**Fig. 26** 3D plots for incubation time and pH



time (8.1) — n-butyl acetate [52]. This result showed that bioethanol produced from KR:SFW was similar to commercially available chemical grade ethanol. The bioethanol yield was found to be 0.68% (w/w). Recent research indicated a yield of 0.34 g ethanol/g glucose or 67% theoretical yield, which is produced through the pseudostem of *Musa Cavendish* using *Saccharomyces cerevisiae* MTCC 4779 [33]. From above, confirms the KR:SFW can be used as a useful alternative biomass for fermentation industries, for the production of bioethanol.

## 4 Conclusion

The present study revealed the optimization of fermentation parameters such as incubation time (24 to 60 h), pH from 4 to 6, agitation speed (60–120 rpm), and inoculum size (3 to 15 vol%) using RSM for bioethanol yield. The predicted  $R^2$  of 0.97 is in reasonable agreement with the adjusted of  $R^2$  0.98. The kinetic models such as logistic and modified Gombertz models were fitted for bioethanol production and it showed high accuracy of  $R^2 > 0.98$ . The

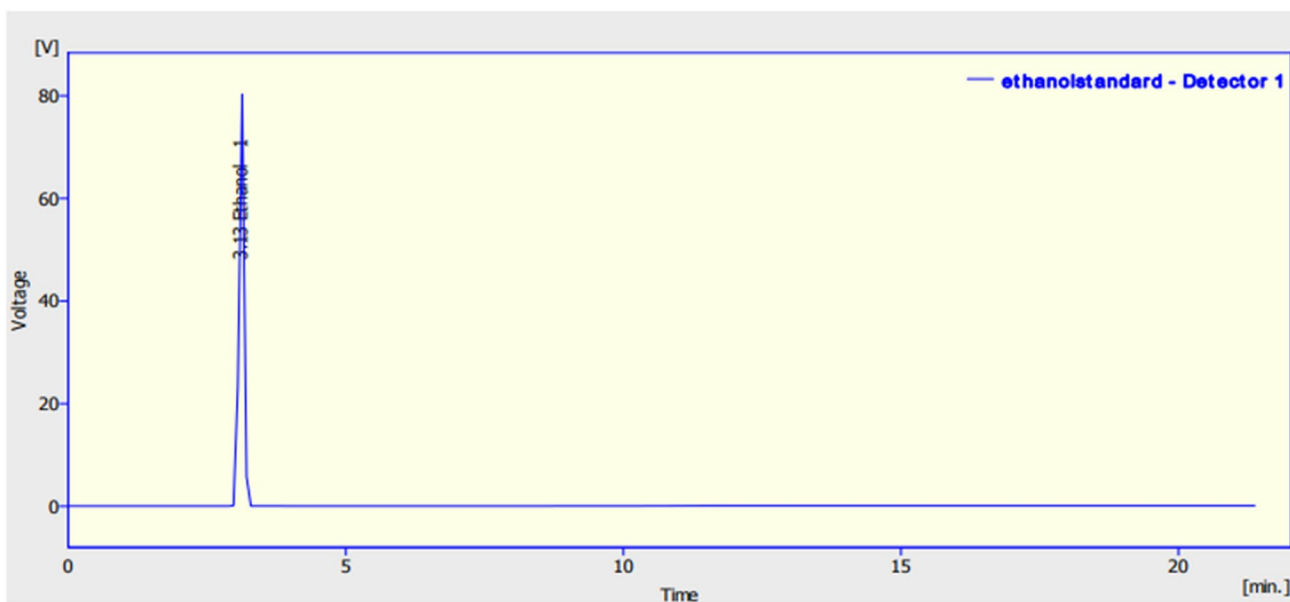
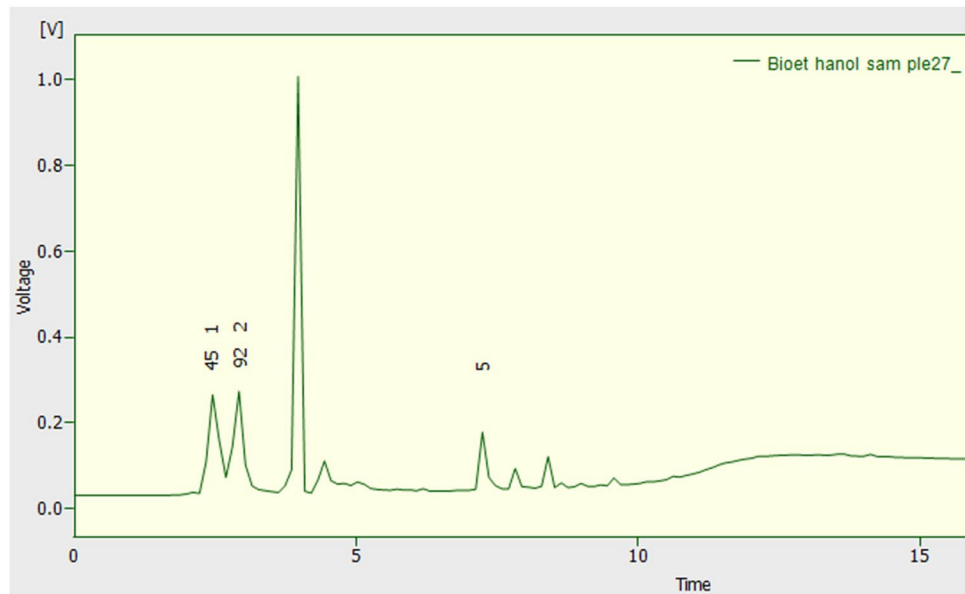


**Fig. 27** GC profile of standard ethanol

**Fig. 28** GC profile of bioethanol produced from KR:SFW sample



optimal conditions are 24 h, 15 (vol%) inoculum size, pH 5, and 90 agitation speed (rpm) for maximum bioethanol yield of 0.68% (w/w). These experimental results provide substantial knowledge about effective utilization of KR:SFW for bioethanol production.

**Supplementary Information** The online version contains supplementary material available at <https://doi.org/10.1007/s13399-021-01819-w>.

**Acknowledgements** The authors thank the Department of Chemistry, Sathyabama Institute of Science and Technology, for using rotary evaporator (SA-RE29T43, SPAN) specialty.

**Funding** The authors thank the Ministry of Human Resource and Development (MHRD, Govt. Of India) Grant No: 5–5/2014-TS. VII 4th September 2014 for financial support in establishing the Centre of Excellence for Energy Research.

## Declarations

**Conflict of interest** The authors declare no competing interests.

## References

- Manilal A, Sujith S, Kiran GS, Selvin J, Shakir C, Gandhimathi R, Panikkar MVN (2009) Biopotentials of seaweeds collected from southwest coast of India. *J Mar Sci Technol* 17:67–73
- Sudhakar MP, Merlyn R, Arunkumar K, Perumal K (2016) Characterization, pretreatment and saccharification of spent seaweed biomass for bioethanol production using baker's yeast. *Biomass Bioenerg* 90:148–154
- Packiyadhas P, Shanmuganantham Selvanantham D (2020) Compositional and structural evaluation of *Kappaphycus alvarezii* rejects and solid food waste blends for bio ethanol production. *Energy Sources Part A Recover Util Environ Eff* 42:1–17
- Khambhaty Y, Mody K, Gandhi MR, Thampy S, Maiti P, Brahmhatt H, Eswaran K, Ghosh PK (2012) *Kappaphycus alvarezii* as a source of bioethanol. *Bioresour Technol* 103:180–185
- Wang Q, Ma H, Wang X, Ji Y (2004) Resource recycling technology of food wastes. *Mod Chem Ind* 24:56–59
- Kiran EU, Liu Y (2015) Bioethanol production from mixed food waste by an effective enzymatic pretreatment. *Fuel* 159:463–469
- Tanaka M, Ozaki H, Ando A, Kambara S, Moritomi H (2008) Basic characteristics of food waste and food ash on steam gasification. *Ind Eng Chem Res* 47:2414–2419
- Okonko IO, Adeola OT, Aloysius FE, Damilola AO, Adewale OA (2009) Utilization of food wastes for sustainable development. *Electron J Environ Agric Food Chem* 8:263–286
- McMillan JD (1997) Bioethanol production: status and prospects. *Renew Energy* 10:295–302
- Islam MN, Park K-J, Yoon H-S (2012) Methane production potential of food waste and food waste mixture with swine manure in anaerobic digestion. *J Biosyst Eng* 37:100–105
- Zhu T, Curtis J, Clancy M (2019) Promoting agricultural biogas and biomethane production: Lessons from cross-country studies. *Renew Sustain Energy Rev* 114:109332
- Qyyum MA, Haider J, Qadeer K, Valentina V, Khan A, Yasin M, Aslam M, De Guido G, Pellegrini LA, Lee M (2020) Biogas to liquefied biomethane: assessment of 3P's—production, processing, and prospects. *Renew Sustain Energy Rev* 119:109561
- Hou T, Zhao J, Lei Z, Shimizu K, Zhang Z (2020) Synergistic effects of rice straw and rice bran on enhanced methane production and process stability of anaerobic digestion of food waste. *Bioresour Technol* 314:123775
- Krithiga T, Sabina XJ, Rajesh B, Ilbeygi H, Shetty AN, Reddy R, Karthikeyan J (2018) Cooked food waste—an efficient and less expensive precursor for the generation of activated carbon. *J Nanosci Nanotechnol* 18:4106–4113
- Sophanodorn K, Unpaprom Y, Whangchai K, Duangsuphasin A, Manmai N, Ramaraj R (2020) A biorefinery approach for the production of bioethanol from alkaline-pretreated, enzymatically hydrolyzed *Nicotiana tabacum* stalks as feedstock for the bio-based industry. *Biomass Convers Biorefinery* 2:1–9
- Casabar JT, Unpaprom Y, Ramaraj R (2019) Fermentation of pineapple fruit peel wastes for bioethanol production. *Biomass Convers Biorefinery* 9:761–765

17. Kadimpati KK, Thadikamala S, Devarapalli K, Banoth L, Uppuluri KB (2021) Characterization and hydrolysis optimization of *Sargassum cinereum* for the fermentative production of 3G bioethanol. *Biomass Convers Biorefinery* 2:1–11
18. Sudhakar MP, Arunkumar K, Perumal K (2020) Pretreatment and process optimization of spent seaweed biomass (SSB) for bioethanol production using yeast (*Saccharomyces cerevisiae*). *Renew Energy* 153:456–471
19. Han W, Liu Y, Xu X, Huang J, He H, Chen L, Qiu S, Tang J, Hou P (2020) Bioethanol production from waste hamburger by enzymatic hydrolysis and fermentation. *J Clean Prod* 264:121658
20. Emiroğlu AO, Şen M (2018) Combustion, performance and emission characteristics of various alcohol blends in a single cylinder diesel engine. *Fuel* 212:34–40
21. Dhande DY, Sinaga N, Dahe KB (2021) Study on combustion, performance and exhaust emissions of bioethanol-gasoline blended spark ignition engine. *Heliyon* 7:e06380
22. Betiku E, Taiwo AE (2015) Modeling and optimization of bioethanol production from breadfruit starch hydrolyzate vis-à-vis response surface methodology and artificial neural network. *Renew Energy* 74:87–94
23. Manmai N, Unpaprom Y, Ramaraj R (2020) Bioethanol production from sunflower stalk: application of chemical and biological pretreatments by response surface methodology (RSM). *Biomass Convers Biorefinery* 3:1–15
24. Thongdumy P, Intrasungkha N, Sompong O (2014) Optimization of ethanol production from food waste hydrolysate by co-culture of *Zymomonas mobilis* and *Candida shehatae* under non-sterile condition. *African J Biotechnol* 13:866–873
25. Castillo FJ, Izaguirre ME, Michelena V, Moreno B (1982) Optimization of fermentation conditions for ethanol production from whey. *Biotechnol Lett* 4:567–572
26. Chouaibi M, Ben Daoued K, Riguane K, Rouissi T, Ferrari G (2020) Production of bioethanol from pumpkin peel wastes: comparison between response surface methodology (RSM) and artificial neural networks (ANN). *Ind Crops Prod* 155:112822
27. Rudke AR, de Andrade CJ, Ferreira SRS (2020) *Kappaphycus alvarezii* macroalgae: an unexplored and valuable biomass for green biorefinery conversion. *Trends Food Sci Technol* 103:214–224
28. Sharma P, Gaur VK, Sirohi R, Varjani S, Kim SH, Wong JWC (2021) Sustainable processing of food waste for production of bio-based products for circular bioeconomy. *Bioresour Technol* 325:124684
29. Tun MM, Juchelková D, Tun MM, Juchelková D (2018) Drying methods for municipal solid waste quality improvement in the developed and developing countries: a review. *Environ Eng Res* 24:529–542
30. Markou G, Angelidaki I, Nerantzis E, Georgakakis D (2013) Bioethanol production by carbohydrate-enriched biomass of *Arthrospira* (*Spirulina*) *platensis*. *Energies* 6:3937–3950
31. Chala B, Oechsner H, Müller J (2019) Introducing temperature as variable parameter into kinetic models for anaerobic fermentation of coffee husk, pulp and mucilage. *Appl Sci* 9:412
32. Samsudin MDM, Don MM, Ibrahim N, Kasmani RM, Zakaria Z, Kamarudin KS (2017) Batch fermentation of bioethanol from the residues of *Elaeis guineensis*: optimisation using response surface methodology. *Chem Eng Trans* 56:1579–1584
33. Seenivasan M, Sanjayini SJ, Kumar MA, Vinodhini G, Hellen Sathya J, Kumar VV (2017) Cellulase-mediated saccharification of lignocellulosic-rich pseudostem of *Musa cavendish* for bioethanol production by *Saccharomyces cerevisiae* MTCC 4779. *Energy Sources Part A Recover Util Environ Eff* 39:570–575
34. Ahmad N, Sahrin N, Talib N, Ghani FSA (2019) Characterization of energy content in food waste by using thermogravimetric analyser (TGA) and elemental analyser (CHNS-O). In: *J Phys Conf Ser*, IOP Publishing, 1349:12140
35. Ye N, Li D, Chen L, Zhang X, Xu D (2010) Comparative studies of the pyrolytic and kinetic characteristics of maize straw and the seaweed *Ulva pertusa*. *PLoS One* 5:e12641
36. Amuzu-Sefordzi B, Huang J, Gong M (2014) Hydrogen production by supercritical water gasification of food waste using nickel and alkali catalysts. *WIT Trans Ecol Environ* 190:285–296
37. Tesfaw A, Assefa F (2014) Current trends in bioethanol production by *Saccharomyces cerevisiae*: substrate, inhibitor reduction, growth variables, coculture, and immobilization. *Int Sch Res Not* 2014:1–11
38. Boudjema K, Fazouane-Naimi F, Hellal A (2015) Optimization of the bioethanol production on sweet cheese whey by *Saccharomyces cerevisiae* DIV13-Z087C0VS using response surface methodology (RSM). *Rom Biotech Lett* 20:10814–10825
39. Sharma N, Kalra KL, Oberoi HS, Bansal S (2007) Optimization of fermentation parameters for production of ethanol from kinnow waste and banana peels by simultaneous saccharification and fermentation. *Indian J Microbiol* 47:310–316
40. Alfenore S, Cameleyre X, Benbadis L, Bideaux C, Uribelarrea J-L, Goma G, Molina-Jouve C, Guillouet SE (2004) Aeration strategy: a need for very high ethanol performance in *Saccharomyces cerevisiae* fed-batch process. *Appl Microbiol Biotechnol* 63:537–542
41. de Albuquerque Wanderley AC, Soares ML, Gouveia ER (2014) Selection of inoculum size and *Saccharomyces cerevisiae* strain for ethanol production in simultaneous saccharification and fermentation (SSF) of sugar cane bagasse. *Afr J Biotechnol* 13:2762–2765
42. Sewsynker-Sukai Y, Kana EBG (2018) Simultaneous saccharification and bioethanol production from corn cobs: process optimization and kinetic studies. *Bioresour Technol* 262:32–41
43. Phukoetphim N, Salakkam A, Laopaiboon P, Laopaiboon L (2017) Kinetic models for batch ethanol production from sweet sorghum juice under normal and high gravity fermentations: logistic and modified Gompertz models. *J Biotechnol* 243:69–75
44. Chohan NA, Aruwajoye GS, Sewsynker-Sukai Y, Kana EBG (2020) Valorisation of potato peel wastes for bioethanol production using simultaneous saccharification and fermentation: process optimization and kinetic assessment. *Renew Energy* 146:1031–1040
45. Sebayang AH, Masjuki HH, Ong HC, Dharma S, Silitonga AS, Kusumo F, Milano J (2017) Optimization of bioethanol production from sorghum grains using artificial neural networks integrated with ant colony. *Ind Crops Prod* 97:146–155
46. Moodley P, Kana EBG (2019) Bioethanol production from sugarcane leaf waste: effect of various optimized pretreatments and fermentation conditions on process kinetics. *Biotechnol Rep* 22:e00329
47. Tarangini K, Kumar A, Satpathy GR, Sangal VK (2009) Statistical optimization of process parameters for Cr (VI) biosorption onto mixed cultures of *Pseudomonas aeruginosa* and *Bacillus subtilis*. *Clean-Soil, Air, Water* 37:319–327



48. Feng Y, Cai Z, Li H, Du Z, Liu X (2013) Response surface optimization of fluidized roasting reduction of low-grade pyrolusite coupling with pretreatment of stone coal. *J Min Metall B Metall* 49:33–41
49. Jayaprabakar J, Dawn SS, Ranjan A, Priyadharsini P, George RJ, Sadaf S, Rajha CR (2019) Process optimization for biodiesel production from sheep skin and its performance, emission and combustion characterization in CI engine. *Energy* 174:54–68
50. El-Gendy NS, Madian HR, Amr SSA (2013) Design and optimization of a process for sugarcane molasses fermentation by *Saccharomyces cerevisiae* using response surface methodology. *Int J Microbiol* 2013:1–9
51. Baş D, Boyacı IH (2007) Modeling and optimization I: Usability of response surface methodology. *J Food Eng* 78:836–845
52. Tiscione NB, Alford I, Yeatman DT, Shan X (2011) Ethanol analysis by headspace gas chromatography with simultaneous flame-ionization and mass spectrometry detection. *J Anal Toxicol* 35:501–511

**Publisher's note** Springer Nature remains neutral with regard to jurisdictional claims in published maps and institutional affiliations.